Instability of a Landau Fermi liquid as the Mott insulator is approached

N. Furukawa* **and T.M.Rice**

Theoretische Physik, ETH-Hönggerberg,
CH-8093 Zürich, Switzerland

Abstract We examine a two-dimensional Fermi liquid with a Fermi surface which touches the Umklapp surface first at the 4 points $(\pm\pi/2,\ \pm\pi/2)$ as the electron density is increased. Umklapp processes at the 4 patches near $(\pm\pi/2,\ \pm\pi/2)$ lead the renormalization group equations to scale to strong coupling resembling the behavior of a 2-leg ladder at half-filling. The incompressible character of the fixed point causes a breakdown of Landau theory at these patches. A further increase in density spreads the incompressible regions so that the open Fermi surface shrinks to 4 disconnected segments. This non-Landau state, in which parts of the Fermi surface are truncated to form an insulating spin liquid, has many features in common with phenomenological models recently proposed for the cuprate superconductors.

* Permanent Address:
Institute for Solid State Physics, Univ. of Tokyo, Minato-ku, Tokyo 106-8666, Japan.

One of the key issues in high-T_c superconductivity is the nature of the anomalous normal state which shows many indices of non-Landau-Fermi liquid behavior. This contrasts with the behavior of many other transition metal oxides which have strongly renormalized Landau-Fermi liquids near to the Mott transition but no superconductivity [1]. Haldane [2] has shown that Landau theory is generally valid in two dimensions. This has led to a search for some instability of the Fermi liquid with increasing electron density in the overdoped cuprates. In this letter we show how Umklapp scattering can cause an instability of the Fermi surface of a 2-dimensional metal as the Mott state is approached. This instability need not involve long range magnetic order but it causes a charge gap and truncation of parts of the Fermi surface. This type of behavior has been documented in a lightly doped 3-leg ladder where the two even parity channels form an insulating spin liquid (ISL) leaving a Fermi surface only in the odd parity channel [3, 4]. Here we discuss how a similar behavior can arise in two dimensions.

We start with a general 2-dim. dispersion relation, for example a form, $\varepsilon(\mathbf{k}) = -2t(\cos k_x + \cos k_y) - 4t' \cos k_x \cos k_y$ with $t(t')$ as (next) nearest neighbor hopping matrix elements. Taking $t > 0$ and $t' > 0$ and increasing the electron density, n, leads to a Fermi surface which touches the surface at which Umklapp processes are allowed first at the 4 points $(\pm\pi/2,\ \pm\pi/2)$. Following Haldane [2] we divide the Fermi surface into patches and examine the patches near the 4 points $(\pm\pi/2,\ \pm\pi/2)$. These 4 patches on the Fermi surface are connected through Umklapp processes which leads us to examine the renormalization group (RG) equations for the coupling constants. The RG equations have similarities to those for a 2-leg ladder at half-filling which also has 4 Fermi surface points and which are known to scale to a strong coupling solution.

The 4 patches around $(\pm\pi/2,\ \pm\pi/2)$ are sketched in Fig. 1. The size of a patch is defined by a wavevector cutoff, k_c, and within each patch $\alpha(\alpha = 1, \ldots, 4)$ the electron

energy relative to the chemical potential, μ is expanded as

$$\varepsilon_\alpha(\mathbf{q}) - \mu = vq_\alpha + uq_{\perp,\alpha}^2 \tag{1}$$

where $\mathbf{q}$ is the wavevector measured from the center of α-th patch, and q_α ($q_{\perp,\alpha}$) is the component of $\mathbf{q}$ normal (tangent) to the Fermi surface at the center of the patch. The Fermi velocity is given by v, and the energy cutoff is $E_0 = vk_c$. We define $v^* = \pi v/k_c$, and hereafter take $\pi v^* = 1$ as the unit of energy.

The linear dispersion relation leads to logarithmic anomalies in the particle-hole (Peierls) and particle-particle (Cooper) channels as in one dimension but the transverse dispersion introduces an infrared cutoff, E_T, with a magnitude $E_T \approx uk_c^2$. The non-interacting susceptibility in the Peierls channel takes the form $\chi_p(\omega) = 1/2\ln(\max(\omega, E_T)/E_c)$. In the parameter region $\omega > E_T$, the infrared cutoff from the transverse dispersion can be ignored and a set of RG equations can be derived as in one dimension [5].

In Fig. 2 we define the normal vertices g_1, g_2 and $g_{1\mathrm{r}}$ as well as Umklapp vertices g_3, $g_{3\mathrm{p}}$ and $g_{3\mathrm{x}}$. Other interactions are not treated here since they are irrelevant within the framework of a one-loop approximation. Summing up all one-loop diagrams, we obtain the RG equations

$$\begin{aligned}
\dot{g}_1 &= {g_1}^2 + {g_{1\mathrm{r}}}^2 + 2{g_{3\mathrm{x}}}^2 - 2g_{3\mathrm{x}}g_{3\mathrm{p}}, && (2)\\
\dot{g}_2 &= \frac{1}{2}({g_1}^2 + 2{g_{1\mathrm{r}}}^2 - g_3^2 - 2{g_{3\mathrm{p}}}^2), && (3)\\
\dot{g}_{1\mathrm{r}} &= (g_1 + g_2)g_{1\mathrm{r}}, && (4)\\
\dot{g}_3 &= (g_1 - 2g_2)g_3 + 2{g_{3\mathrm{x}}}^2 - 2g_{3\mathrm{x}}g_{3\mathrm{p}} - {g_{3\mathrm{p}}}^2, && (5)\\
\dot{g}_{3\mathrm{x}} &= 2g_1g_{3\mathrm{x}} - g_1g_{3\mathrm{p}} - g_2g_{3\mathrm{x}} + g_3g_{3\mathrm{x}} - g_3g_{3\mathrm{p}}, && (6)\\
\dot{g}_{3\mathrm{p}} &= -(g_2 + g_3)g_{3\mathrm{p}}. && (7)
\end{aligned}$$

Here $\dot{g}_i \equiv x(\mathrm{d}g_i)/(\mathrm{d}x)$ and $x = \omega/E_0$.

Note these equations differ from those obtained by Zheleznyak *et al.* [6] who earlier considered a model with 4 flat Fermi surface patches. In their model the patches were

oriented perpendicular to the (1,0) and (0,1) directions and as a consequence Umklapp processes connecting perpendicular patches did not enter the RG equations which are then more closely related to those for a single chain at half-filling. Eqns. (2-7) coincide with those derived previously by Houghton and Marston [7] who considered the problem of a lightly doped flux state rather than the present limit of a heavily doped model with next-nearest-neighbor hopping.

We take repulsive Umklapp interactions, as $g_3 = g_{3\mathrm{x}} = g_{3\mathrm{p}} = U$, and treat g_1, g_2 and $g_{1\mathrm{r}}$ as parameters. The fixed points are obtained by numerically integrating the RG equations. In a substantially wide region around $g_1 \sim g_2 \sim g_{1\mathrm{r}} \sim U$, we find a strong coupling fixed point where both normal and Umklapp vertices diverge. The corresponding phase diagram is shown in Fig. 3. The asymptotic behavior of the vertices is given by $g_i = g_i^0 \Lambda/[1 + \Lambda \log(\omega/E_0)]$, where $(g_1^0, g_2^0, g_{1\mathrm{r}}^0, g_3^0, g_{3\mathrm{p}}^0, g_{3\mathrm{x}}^0) = (\frac{1}{14}, \frac{5}{14}, 0, \frac{9}{14}, \frac{1}{7}\sqrt{\frac{15}{2}}, \frac{1}{14}\sqrt{\frac{15}{2}})$. A singularity appears at $\omega \sim \omega_c = E_0 \exp(-1/\Lambda)$ where $\Lambda \propto U$. In two dimensions, such an anomaly at finite ω is an artifact of the one-loop calculation and higher order terms will shift it to $\omega = 0$. Nevertheless, ω_c represents the energy scale where the system crosses over from weak coupling to strong coupling. We will explicitly assume that the interactions $\sim U$ are strong enough so that $\omega_c > E_T$ in which case the existence of a finite curvature becomes irrelevant at the strong coupling fixed point. In contrast, if the system had scaled to weak coupling, then E_T would always remain relevant. There is a limit with weak interactions and a dispersion relation with $t' \ll t$ where both conditions, $E_T (= 2t'k_c^2) \ll \omega_c$ and $U \ll E_0$, are satisfied and our approach based on one-loop RG equations is justified. We speculate that the qualitative nature of the anomaly obtained in this weak coupling region is also present in the strong coupling region $U \gtrsim t, t'$.

We now discuss the nature of the fixed point through the anomalies in the susceptibilities. Due to the nesting behavior in the non-interacting case, there may exist anomalies in the spin susceptibility (χ_{s}) and the charge susceptibility (χ_{c}) at $q = (\pi, \pi)$. Within the

one-loop calculation, we find

$$\chi_{\rm s}(\pi,\pi) \propto (\omega-\omega_{\rm c})^{\alpha_{\rm s}}, \quad \alpha_{\rm s}=-g_2^0-g_3^0-2g_{3\rm p}^0, \tag{8}$$

$$\chi_{\rm c}(\pi,\pi) \propto (\omega-\omega_{\rm c})^{\alpha_{\rm c}}, \quad \alpha_{\rm c}=2g_1^0-g_2^0+g_3^0-2g_{3\rm p}^0+4g_{3\rm x}^0. \tag{9}$$

The superconducting susceptibilities for s-, p- and d-wave pairing (Δ_s, Δ_p and Δ_d, respectively) also behave as

$$\Delta_s \propto (\omega-\omega_{\rm c})^{\alpha_{\rm ss}}, \quad \alpha_{\rm ss}=g_2^0+g_1^0+2g_{1\rm r}^0, \tag{10}$$

$$\Delta_p \propto (\omega-\omega_{\rm c})^{\alpha_{\rm ps}}, \quad \alpha_{\rm ps}=g_2^0-g_1^0, \tag{11}$$

$$\Delta_d \propto (\omega-\omega_{\rm c})^{\alpha_{\rm ds}}, \quad \alpha_{\rm ds}=g_2^0+g_1^0-2g_{1\rm r}^0. \tag{12}$$

At the fixed point with strong Umklapp coupling described above, the leading divergence is observed in the spin susceptibility with the exponent $\alpha_{\rm s}=-1.782$, while the exponents for charge and superconducting susceptibilities are positive so that these susceptibilities do not diverge at the critical point.

The uniform spin ($\chi_s(0)$) and charge (κ) [8, 9] susceptibilities are also of interest. As in the case of 1d chain system, we have spin gap behavior when there is a divergence in g_1 and charge gap behavior from g_3,

$$\chi_{\rm s}(0) \propto (\omega-\omega_{\rm c})^{(g_1^0)^2/2}, \tag{13}$$

$$\kappa \propto (\omega-\omega_{\rm c})^{(g_3^0)^2/4}. \tag{14}$$

Here we approach $\omega_{\rm c}$ by decreasing both ω and q with q/ω being fixed. In the present case, both g_1 and g_3 flow to strong coupling which indicates a tendency to open up both spin and charge gaps.

We now compare the present results to those of a two-leg ladder at half-filling. In this case, as Balents and Fisher have shown [10], there are 9 vertices which are relevant within a one-loop calculation. Again the flow is to strong coupling in backward and Umklapp

scattering channels. In this case the properties of the strong coupling fixed point are well established. The system is an insulating spin liquid (ISL) with both spin and charge gaps (C0S0 in the Balents-Fisher notation) and is an example of a short range RVB (Resonant Valence Bond) state first proposed by Anderson for a $S = 1/2$ Heisenberg model [11]. The spin susceptibility $\chi_s(\pi, \pi)$ is strongly enhanced but remains finite.

In the present case we cannot be sure of the spin properties from the one-loop calculations especially since the spin susceptibility at (π, π) and $(0, 0)$ behave in a contradictory fashion. What is certain is the scaling to strong coupling with diverging Umklapp scattering. This gives us confidence in the result that the compressibility $\kappa = dk_{F,\alpha}/d\mu \to 0$ at the fixed point as it does in the two-leg ladder at half-filling. This has several profound consequences. First the condensate that forms is pinned and insulating. Secondly when additional electrons are added to the system the Fermi surface does not simply expand along the $(\pm 1, \pm 1)$ directions beyond the $(\pm\pi/2,\ \pm\pi/2)$ points as would happen for non-interacting electrons. Instead the charge gap and vanishing $dk_{F\alpha}/d\mu$ force the additional electrons to be accommodated in the rest of Fermi surface.

Our proposal that the strong coupling fixed point is in the same universality class (C0S0) as that of the two-leg ladder at half-filling differs from the conclusions of Zheleznyak *et al.* [6] who found antiferromagnetic order in their model which in turn is rather related to the class of fixed points of the single chain at half-filling (C0S1). Note that the finite curvature in the present model, which kills nesting properties, acts to suppress the Peierls channel away from the 4 patches and therefore the tendency to antiferromagnetic order. A similar conclusion was reached in ref. [6] when a finite curvature was included.

To examine what happens next we increase the electron density such that there are 8 points on the Umklapp surface which intersect the non-interacting Fermi surface at a finite angle (see Fig. 4a). This leads us to examine an 8-patch model allowing for Umklapp scattering processes. Within a one-loop calculation, the 8-patch model has 9

relevant coupling constants, defined in Fig. 5, and their RG equations are given by

$$\dot{g}_1 = {g_1}^2 + g_{1x}g_{2x} + g_{1s}g_{1l} + {g_{1r}}^2 + {g_{3x}}^2 - g_{3p}g_{3x}, \quad (15)$$

$$\dot{g}_2 = \frac{1}{2}({g_1}^2 + {g_{1x}}^2 + {g_{2x}}^2 + {g_{1s}}^2 + {g_{1l}}^2 + 2{g_{1r}}^2 - {g_{3p}}^2), \quad (16)$$

$$\dot{g}_{1x} = g_1 g_{2x} + g_2 g_{1x} + (g_{1s} + g_{1l})g_{1r}, \quad (17)$$

$$\dot{g}_{2x} = g_1 g_{1x} + g_2 g_{2x} + (g_{1s} + g_{1l})g_{1r}, \quad (18)$$

$$\dot{g}_{1s} = g_1 g_{1l} + g_2 g_{2s} + (g_{1x} + g_{2x})g_{1r}, \quad (19)$$

$$\dot{g}_{1l} = g_1 g_{1s} + g_2 g_{2l} + (g_{1x} + g_{2x})g_{1r}, \quad (20)$$

$$\dot{g}_{1r} = 2(g_1 + g_2)g_{1r} + (g_{1x} + g_{2x})(g_{1s} + g_{1l}), \quad (21)$$

$$\dot{g}_{3p} = -g_2 g_{3p}, \quad (22)$$

$$\dot{g}_{3x} = (2g_1 - g_2)g_{3x} - g_1 g_{3p}. \quad (23)$$

For Hubbard-like interactions, $g_i = U$, numerical integration shows that the interactions flow to a strong coupling fixed point with divergent g_1, g_2, g_{3x} and g_{3p} with prefactors as $g_1^0 = \frac{1}{3}(-2+\sqrt{10})$, $g_2^0 = 1$, and $g_{3p}^0 = 2g_{3x}^0 = \frac{2}{3}\sqrt{8-\sqrt{10}}$, while the other couplings flow to zero. Examining the susceptibilities gives us again the result that the spin susceptibility diverges most strongly with an exponent $\alpha_s = -g_2^0 = -1$. However the wavevector is no longer (π, π) but the incommensurate wavevector connecting patches that span the Fermi surface. The uniform spin susceptibility $\chi_s(0)$ diverges to zero but the compressibility κ is not renormalized to this order.

The scaling of the one-loop equations to a strong coupling fixed point, even when we start with a non-interacting Fermi surface, makes it necessary to consider the strong coupling behavior further. The restriction that we found in the 4-patch model, which prevents the Fermi wavevector along $(\pm 1, \pm 1)$ directions from extending past the Umklapp surface, strongly suggests that this behavior will spread out laterally as indicated in Fig. 4b. Again we can draw a parallel to the slightly doped 3-leg ladder where in strong coupling a C1S1 phase containing an ISL with commensurate filling in the even parity

channels remains stable up to a critical density. This contrasts with the one-loop result which gives a C2S1 phase with holes immediately entering both odd and even-parity channels. Actually we can examine the strong coupling limit self-consistently. If we start from a dispersion of the form Fig. 4b in a 8-patch model, then we find that $\kappa \to 0$. So a lateral spreading of the truncated region of the Fermi surface, as shown in Fig. 4b, is self-consistent.

While a one-loop calculation is of limited validity at a strong coupling fixed point, there are a number of conclusions that can be drawn. First the breakdown of Landau theory, as the system scales to a fixed point with strong Umklapp scattering is certain. Less certain is the question whether it has long range spin order or not. Even if it has, it is not the essence of the fixed point, which is the divergence of Umklapp scattering as the fixed point is approached. The most likely form remains an ISL spreading across the Fermi surface which successively truncates the Fermi surface as shown schematically in Fig. 4b. This is consistent with the result that $\chi_s(0) \to 0$ always. The condensate is pinned and insulating due to the Umklapp scattering. We note that an ISL, which truncates part of the Fermi surface, is not characterized by any simple broken symmetry or order parameter. It is not amenable to a simple mean field or Hartree-Fock theory since there are no anomalous averages. Also the onset of the ISL is a crossover rather than a phase transition at finite temperature. Lastly we should remark that the ISL is not incompressible since it can expand or contract laterally by exchanging electrons with the open parts of the Fermi surface.

The Fermi surface in the cuprates has a different form with $t' < 0$ and not $t' > 0$ as we investigated. In this case the Fermi surface first touches the Umklapp surface at the saddle points $(\pi, 0)$ and $(0, \pi)$. This leads to complications in the analysis due to the presence of $\ln^2(\omega/E_0)$ terms in the RG equations which will require additional analysis in the future. Dzyaloshinskii [12] has made a detailed analysis of a weak coupling fixed point for this

model leading to a form of Luttinger liquid behavior. Our result for the 8-patch model lead us to consider rather possible strong coupling fixed points with divergent Umklapp scattering which would introduce a charge gap at the Fermi surface. The open Fermi surface will then be 4 disconnected segments centered on $(\pm\pi/2,\ \pm\pi/2)$ as sketched in Fig. 4c, which is similar to the results of a recent SU(2) gauge theory calculation [13]. Signs of such behavior are also evident in a recent analysis of the momentum distribution using a high temperature series by Putikka *et al.* [14]. Note they include only nearest-neighbor terms in the kinetic energy (*i.e.* $t' = 0$) which is a special limit from the present point of view.

If we accept the premise that in the cuprates Umklapp scattering stabilizes an ISL in the vicinity of the saddle points, then there are some interesting consequences. For example, the ISL provides a microscopic justification for some phenomenological models. Geshkenbein, Ioffe and Larkin [15] proposed a model of preformed pairs in the vicinity of the saddle point but with a very large mass to suppress their contribution to the conductivity in the normal phase. Similarly the ISL can provide a reservoir of pairs that act to induce superconductivity in the open parts of the Fermi surface but with the difference that here electron pairs cannot be scattered into the ISL, only hole pairs. In fact experience with the ISL in the 2-leg ladder shows that it is preferable energetically to add holes in pairs to an ISL. Such processes will then by an efficient mechanism cause pairing on the open segments of the Fermi surface. Also recently Murakami and Fukuyama [16] included Umklapp scattering in a mean field treatment and found that it enhanced $d_{x^2-y^2}$-pairing. In the normal state there is a close similarity to a phenomenological model proposed by Ioffe and Millis [17], to explain the anomalous transport properties. Here also the Fermi surface segments have usual quasi-particle properties (i.e. there is no spin-charge separation) and the scattering rate will vary strongly since Umklapp processes will lead to strong scattering at the end of the segments where they meet the Umklapp

surface. These are key features of the phenomenological Ioffe-Millis model. Ioffe and Millis justified their model by a comparison to the tunneling and ARPES experiments [18, 19] which show a single particle gap opening in the vicinity of the saddle points similar to the form in Fig. 4c. Lastly we refer the reader to the very recent preprint by Balents, Fisher and Nayak [20] which introduces the concept of a Nodal liquid with properties similar to the ISL discussed above.

In conclusion we have shown that when the Fermi surface approaches the Umklapp surface, the addition of Umklapp scattering can cause a breakdown of Landau theory. The Fermi surface is truncated by the formation of a pinned and insulating condensate. We have given arguments that the spin properties are those of an insulating spin liquid. This microscopic model has a lot in common with some recent phenomenological models so that we believe it can form the basis for a theory of the cuprates.

Acknowledgments

We wish to thank S. Haas, D. Khveshchenko, M. Sigrist and E. Trubowitz for stimulating conversations.

N.F. is supported by a Monbusho Grant for overseas research.

References

[**1**] M. Imada, A. Fujimori and Y. Tokura, Rev. Mod. Phys, in press.

[**2**] F.D.M. Haldane, in Proc. of the International School of Physics "Enrico Fermi", Course 121, 1992, ed. J.R. Schrieffer and R.A. Broglia (North Holland, New York, 1994). See also J. Fröhlich and R. Götschmann, Phys. Rev. B**55**, 6788 (1997).

[**3**] T.M. Rice, S. Haas, M. Sigrist and F.C. Zhang, Phys. Rev. B**56** 14655 (1997).

[**4**] S.R. White and D.J. Scalapino, Phys. Rev. B**57**, 3031 (1998).

[**5**] J. Sólyom, Adv. in Phys. **28**, 201 (1979).

[**6**] A. T. Zheleznyak, V. M. Yakovenko and I. E. Dzyaloshinskii, Phys. Rev. B**55**, 3200 (1997).

[**7**] A. Houghton and J. B. Marston, Phys. Rev. B48, 7790 (1993).

[**8**] H. Fukuyama, T.M. Rice, C.M. Varma and B.I. Halperin, Phys. Rev. B**10**, 3775 (1974).

[**9**] M. Kimura, Prog. Theo. Phys. **53**, 955 (1975).

[**10**] L. Balents and M.P.A. Fisher, Phys. Rev. B**53**, 12133 (1996); H.-H. Lin, L. Balents and M.P.A. Fisher, Phys. Rev. B**56**, 6569 (1997).

[**11**] P.W. Anderson, Science **235**, 1196 (1987).

[**12**] I. Dzyaloshinskii, J. Phys. I France **6**, 119 (1996).

[**13**] P. A. Lee and X. G. Wen, Phys. Rev. Lett. **78**, 4111 (1997).

[**14**] W. O. Putikka, M. U. Luchini and R. R. P. Singh, preprint, cond-mat/9803141.

[**15**] V.G. Geshkenbein, L.B. Ioffe and A.I. Larkin, Phys. Rev. B**55**, 3173 (1997).

[**16**] M. Murakami and H. Fukuyama, preprint, cond-mat/9802009.

[**17**] L.B. Ioffe and A.J. Millis, preprint, cond-mat/9801092.

[**18**] Ch. Renner, B. Revaz, J.-Y. Genoud, K. Kadowski and Ø. Fischer, Phys. Rev. Lett. **80**, 149 (1998).

[**19**] A.G. Loeser, Z.-X. Shen, D.S. Dessau, D.S. Marshall, C.H. Park, P. Fournier and A. Kapitulnik, Science, **273**, 325 (1996); H. Ding, T. Yokoya, J.C. Campuzano, T. Takahashi, M. Randeria, M.R. Norman, T. Mochiku, K. Kadowaki and J. Giapintzakis, Nature, **382**, 51 (1996).

[**20**] L. Balents, M. P. A. Fisher and C. Nayak, preprint, cond-mat/9803086.

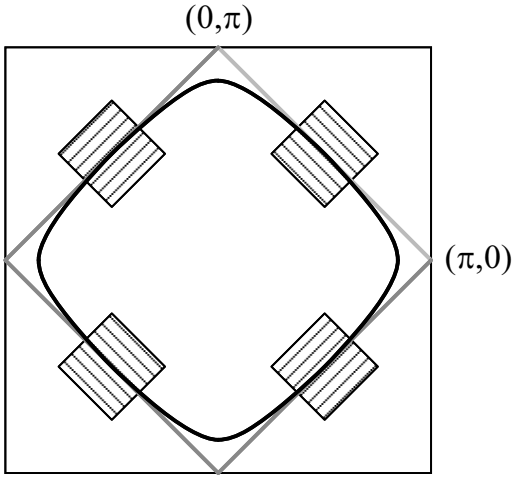

Fig. 1 Furukawa-Rice

Definitions of 4 patches, shown as hatched rectangular areas. The bold curve represents the 2-dimensional Fermi surface which touches the points $(\pm\pi/2, \pm\pi/2)$. The grey lines show the Umklapp surface where Umklapp processes are allowed.

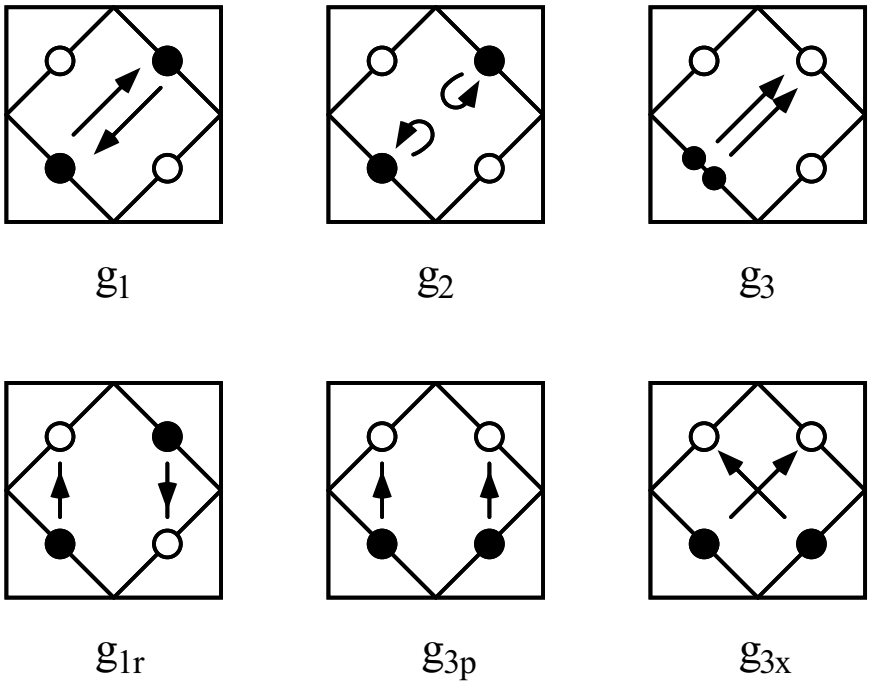

Fig. 2 Furukawa-Rice

The definitions of vertices for the 4-patch model.

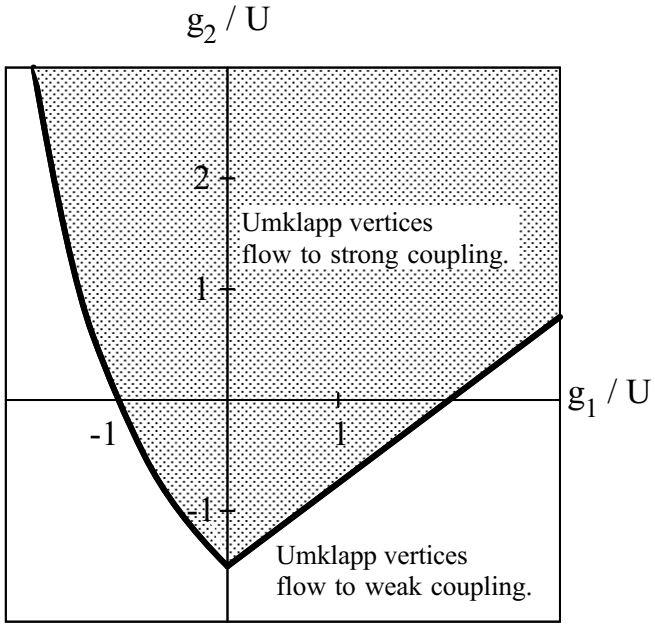

Fig. 3 Furukawa-Rice

Phase diagram of the 4-patch model at $g_3 = g_{3\mathrm{x}} = g_{3\mathrm{p}} = U$. The hatched area shows the region where Umklapp interactions flow to strong coupling. Here, we take $g_{1\mathrm{r}} = g_1$, but the hatched region does not change qualitatively if we take other values for $g_{1\mathrm{r}}$.

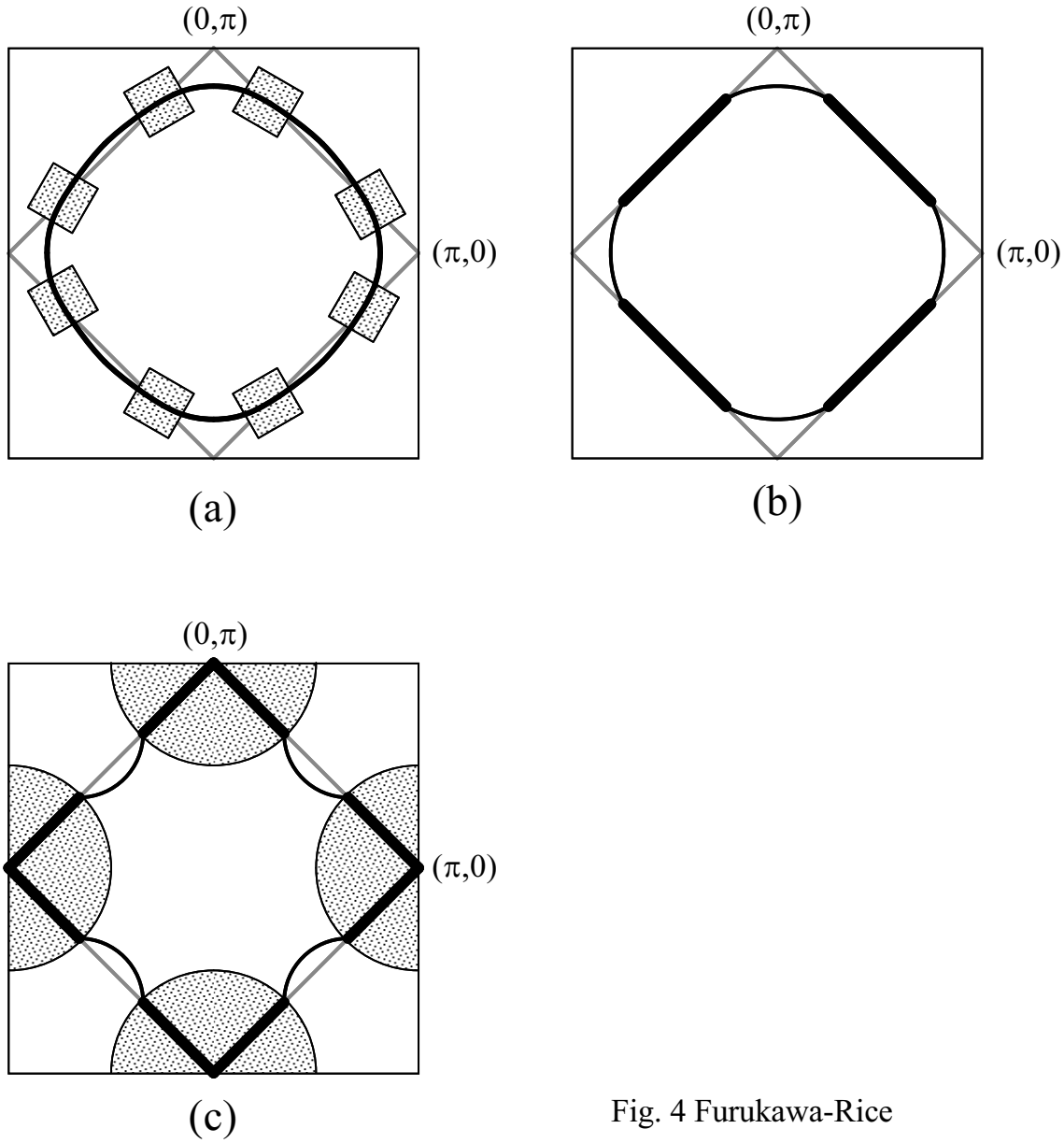

Fig. 4 Furukawa-Rice

Shapes of the Fermi surfaces when electron concentration is further increased. (a) The noninteracting Fermi surface where 8 patches are defined at the intersection with Umklapp surface. (b) The distorted Fermi surface when it is pinned at $(\pm\pi/2, \pm\pi/2)$ points. (c) In the case $t' < 0$, the Fermi surface should be pinned at $(\pi, 0)$ and $(0, \pi)$.

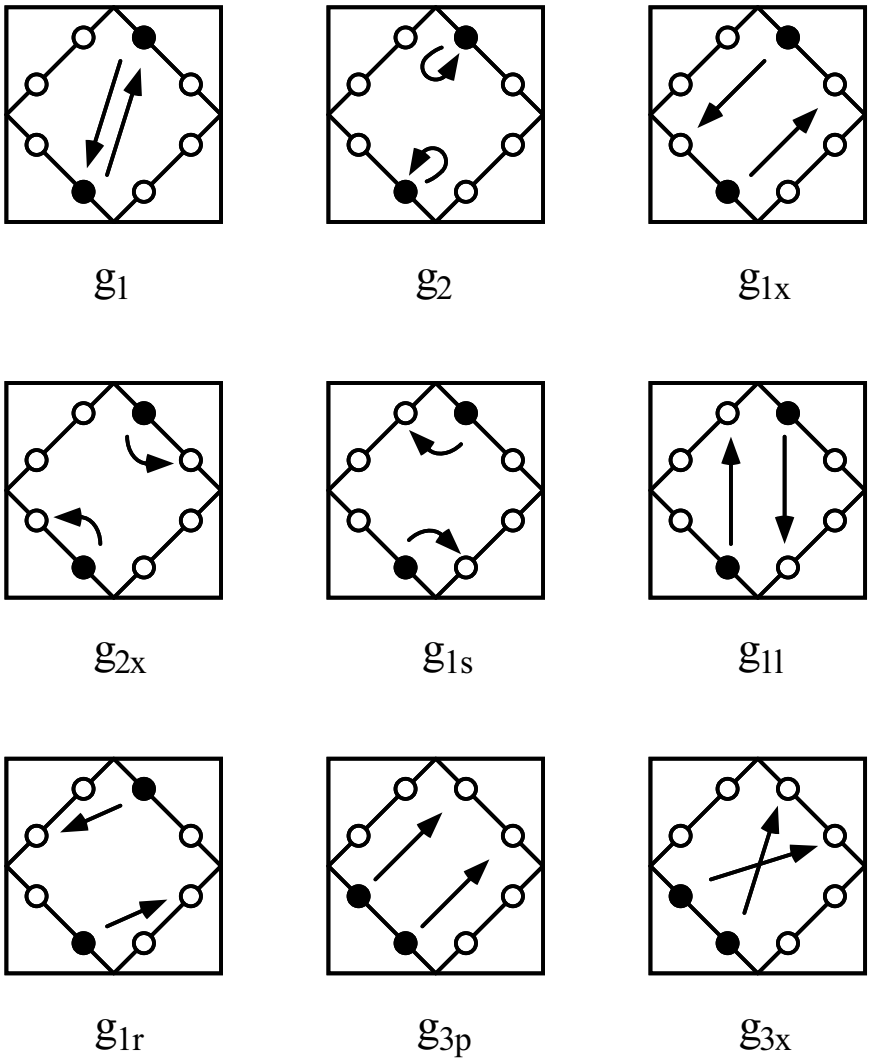

Fig. 5 Furukawa-Rice

The definitions of vertices for the 8-patch model.